J|A|C|S
ARTICLES
Published on Web 09/02/2006

# Methane Dehydrogenation on Rh@Cu(111): A First-Principles Study of a Model Catalyst

Anton Kokalj,*[,†,‡] Nicola Bonini,[†] Stefano de Gironcoli,[†] Carlo Sbraccia,[†] Guido Fratesi,[†] and Stefano Baroni[†]

*Contribution from SISSA—Scuola Internazionale Superiore di Studi Avanzati and CNR-INFM DEMOCRITOS National Simulation Center, I-34014 Trieste, Italy, and Jožef Stefan Institute, SI-1000 Ljubljana, Slovenia*

Received January 6, 2006; E-mail: Tone.Kokalj@ijs.si

***Abstract:*** The issue of tuning the relative height of the first two dehydrogenation barriers of methane ($CH_4 \rightarrow CH_3 + H$ and $CH_3 \rightarrow CH_2 + H$) is addressed using density-functional theory. It is shown that the combination of a very active reaction center—such as Rh—with a more inert substrate—such as Cu(111)—may hinder the second dehydrogenation step with respect to the first, thus resulting in the reverse of the natural order of the two barriers' heights.

## 1. Introduction

Tuning the relative reaction rates of the different steps of methane dehydrogenation would allow for the optimal design of many dream reactions, such as the direct conversions of methane to methanol, formaldehyde, or higher hydrocarbons. The efficiency of transition-metal catalysts to promote these and other related reactions is limited by the tendency of dehydrogenation to proceed until graphite is eventually formed on the surface, thus poisoning the catalyst.[1]

In our recent work,[2] the first two steps of methane dehydrogenation on Rh(111),

$$CH_4 \rightarrow CH_3 + H \qquad \text{and} \qquad (1)$$

$$CH_3 \rightarrow CH_2 + H \qquad (2)$$

were investigated using density-functional theory and focusing on the dependence of the catalyst's reactivity on the atomic coordination ($N_C$) of the active metal center. By comparing the reactivity of defect sites with different atomic coordinations, we found that, while the barrier for the dehydrogenation of methane, (1), decreases as expected with the coordination of the reaction center, the dehydrogenation of methyl, (2), is hindered at an ad-atom defect, where the first reaction is instead most favored. Our findings indicate that, if it were possible to let the dissociation occur selectively at ad-atom defects, the reaction could be blocked after the first dehydrogenation step, a result of high potential interest for many important reactions, such as those mentioned above.

It has long been known that the addition of a group IB metal to group VIII metals can lead to an increased selectivity of the catalyst.[3] In particular, it is known that such catalysts hinder hydrogenolysis reactions, which involve C−C bond breaking, but do not significantly affect dehydrogenation reactions, which involve C−H bond breaking. The selective behavior of bimetallic catalysts is usually described in terms of structural (*ensemble*) and electronic (*ligand*) effects. The *ensemble* effect is defined in terms of the number of surface atoms of a particular type required for a given molecule to bind or adsorb. For example, the hydrogenolysis reaction requires sites with a larger ensemble of active atoms than dehydrogenation reactions. Already the addition of a small amount of a group IB metal will substantially decrease the number of sites composed of large ensembles of active metal atoms, thus making the dehydrogenation reaction more selective.[3] The *ligand* effect refers to modifications of the adsorption or catalytic properties by an electronic effect that results from the interaction between the surface metal atom adsorption site and its neighboring metal atoms. For example, it is known that, in some cases, the addition of an inert group IB metal enhances the adsorption energies on group VIII metals,[4,5] due to an upshift of the d-band center of the active metal. The case of the RhCu alloy has attracted some experimental interest because of its catalytic activity, for example, in the conversion of methane to ethane,[6] in some dehydrogenation reactions,[7] and in NO reduction by CO.[8] These results have also stimulated some theoretical works in which the interaction of NO and CO with this bimetallic system[9,10] and its activity toward $H_2$ dissociation[11] have been studied.

† SISSA and CNR-INFM DEMOCRITOS.
‡ Jožef Stefan Institute.

(1) Gesser, H. D.; Hunter, N. R. *Catal. Today* **1998**, *42*, 183.
(2) Kokalj, A.; Bonini, N.; Sbraccia, C.; de Gironcoli, S.; Baroni, S. *J. Am. Chem. Soc.* **2004**, *126*, 16732.
(3) Sinfelt, J. H. *Bimetallic Catalysts;* John Wiley & Sons: New York, 1983.
(4) Pallassana, V.; Neurock, M. *J. Catal.* **2000**, *191*, 301.
(5) Hammer, B.; Nørskov, J. K. *Surf. Sci.* **1995**, *343*, 211.
(6) Solymosi, F.; Cserényi, J. *Catal. Lett.* **1995**, *34*, 343.
(7) Reyes, P.; Pecchi, G.; Fierro, J. L. G. *Langmuir* **2001**, *17*, 522.
(8) Petrov, L.; Soria, J.; Dimitrov, L.; Cataluña, R.; Spasov, L.; Dimitrov, P. *Appl. Catal. B* **1996,** *8*, 9.
(9) González, S.; Sousa, C.; Illas, F. *Surf. Sci.* **2003**, *531*, 39.
(10) González, S.; Sousa, C.; Illas, F. *J. Phys. Chem. B* **2005**, *109*, 4659.
(11) González, S.; Sousa, C.; Fernández- García, M.; Bertin, V.; Illas, F. *J. Phys. Chem. B* **2005**, *106*, 7839.


**10.1021/ja060114w CCC: $33.50** 

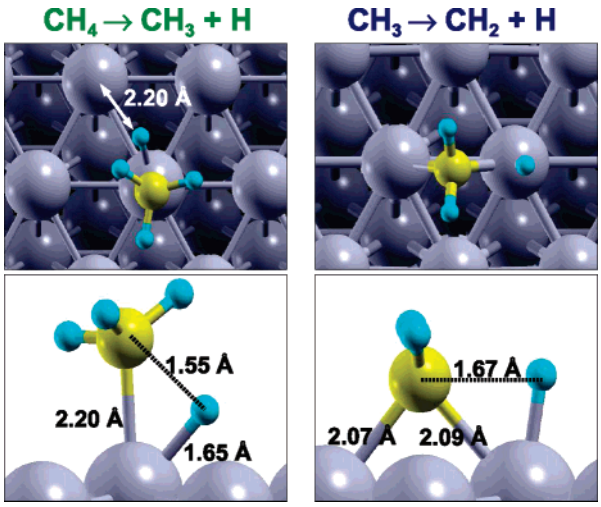


***Figure 1.*** Main features of the transition state (TS) for the first two dehydrogenation reactions on a flat Rh(111) surface.

Encouraged by these considerations and by our previous results, we now extend our investigation by considering the dependence of the catalyst's reactivity on the local chemical composition at the reaction center. In particular, the issue of the reaction selectivity is addressed by considering a reaction center characterized by a reactive atom, such as Rh, on a less reactive substrate, such as Cu(111).

This paper is organized as follows: in section 2 we provide a detailed analysis of the mechanisms responsible for the low reactivity of Rh ad-atom defects toward methyl dehydrogenation.[2] On the basis of this analysis, in section 3 we present the design of a model catalyst in which the selectivity of Rh ad-atom reaction centers is enhanced by embedding them into a less reactive surface, such as Cu(111). Section 4 contains our conclusions, including some considerations on the thermal stability of the model catalyst considered in this paper. Finally, our theoretical and computational frameworks are reviewed in the Supporting Information, Appendix A, while Appendix B therein summarizes the adsorption energies and structural parameters of the various molecular species—methyl, methylene, and hydrogen—considered in this paper.

## 2. Analysis of Reaction Barriers: A Qualitative Understanding

The main features of the transition states (TS) for the two reactions, (1) and (2), on Rh(111) are displayed in Figure 1. (i) For both reactions the TS is *late*, i.e., its structure is close to that of the final state: the C−H distance for the detaching H atom at the TS is in the range 1.6−1.7 Å, to be compared with an equilibrium bond length of 1.1 Å. (ii) The TS of the first reaction, (1), involves only one metal atom: the $CH_3$ fragment is located at the top site, while the dissociating H atom is close to the bridge (or hollow) site. (iii) On the other hand, the TS for the second reaction, (2), involves two metal atoms: the $CH_2$ (*methylene*) fragment is located at the bridge site, while the dissociating H atom is at the top site.

These features for the two TS are not characteristic solely of Rh(111). For example, similar transition states for the first reaction have been observed on Ru(0001),[12] Ni(111),[13,14] and Pd(100).[15] As for the second reaction, two slightly different variants of the TS are reported in the literature. Both TS types

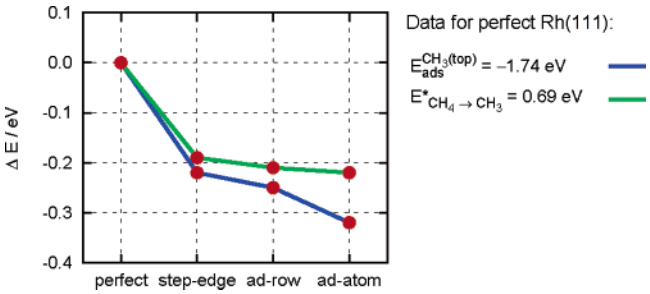


***Figure 2.*** Comparison of the methyl adsorption energies, $E_{chem}$, over a top site (blue line) and activation energies, $E^*$, of the $CH_4 \rightarrow CH_3 + H$ reaction (green line) for different reaction centers. Both quantities are referred to the value they have for the perfect Rh(111) surface.

are characterized by the $CH_2$ and H fragments being located on the bridge and top sites, respectively, but the orientation of methylene is different, according to whether the H−C−H plane is perpendicular or parallel to the bridge (the perpendicular orientation is shown in Figure 1). The parallel orientation of the $CH_2$ fragment was predicted by Ciobica on Ru(0001)[12] and Watwe on Ni(111),[14] whereas Michaelides[16] predicted perpendicular orientation on the same surface. A perpendicular orientation was also predicted by Petersen on Pt(110)(1×2).[17]

**2.1. $CH_4 \rightarrow CH_3 + H$.** The first dehydrogenation of methane has been analyzed in detail by Liu et al.,[18] who showed that the reduction in the activation barrier at less coordinated reaction centers is proportional to the increase of magnitude of the products' ($CH_3$ + H) chemisorption energies. This is typical of late-TS reactions, and also related to the smallness of both the methane binding energy in the initial state and the interaction energy between the fragments in the final state. The H chemisorption energy is rather similar at different reaction centers.[2] Therefore, the reduction of the activation barrier for the first reaction can be most directly related to a stronger $CH_3$−metal bond at less coordinated centers (ligand effect). In Figure 2, we report the adsorption energy of methyl at the top site—the local minimum closest to the $CH_3$ structure at the TS—together with the activation energy for the first dehydrogenation, (1), as a function of the coordination of the active metal center. In particular, four different reaction centers on the (111) surface are considered: a perfect (111) facet ($N_C = 9$), as well as step-edge ($N_C = 7$), ad-row ($N_C = 5$), and ad-atom ($N_C = 3$) defects (see Figure 1 of ref 2). The correlation between the methyl adsorption energies at the top sites and the reaction activation energies is rather good.

**2.2. $CH_3 \rightarrow CH_2 + H$.** In order to perform a similar analysis for the second reaction, (2), let us consider first the reactant, a methyl radical whose unsaturated C atom strongly binds to the metal surface. In addition to this strong bond, methyl also displays a peculiar three-center C−H−metal bond, usually referred to as an *agostic bond* in organometallic chemistry.[19−21]

(12) Ciobica, I. M.; Frechard, F.; van Santen, R. A.; Kleyn, A. W.; Hafner, J. *J. Phys. Chem. B* **2000**, *104*, 3364.
(13) Kratzer, P.; Hammer, B.; Nørskov, J. K. *J. Chem. Phys.* **1996**, *105*, 5595.
(14) Watwe, R. M.; Bengaard, H. S.; Rostrup-Nielsen, J. R.; Dumesic, J. A.; Nørskov, J. K. *J. Catal.* **2000**, *189*, 16.
(15) Zhang, C. J.; Hu, P. *J. Chem. Phys.* **2002**, *116*, 322.
(16) Michaelides, A.; Hu, P. *J. Chem. Phys.* **200**, *112*, 8120.
(17) Petersen, M. A.; Jenkins, S. J.; King, D. A. *J. Phys. Chem. B* **2004**, *108*, 5920.
(18) Liu, Z. P.; Hu, P. *J. Am. Chem. Soc.* **2003**, *125*, 1958.
(19) Zaera, F. *Chem. Rev.* **1995**, *95*, 2651.
(20) Hall, C.; Perutz, R. N. *Chem. Rev.* **1996**, *96*, 3125.
(21) Crabtree, R. H. *Chem. Rev.* **1995**, *95*, 897.

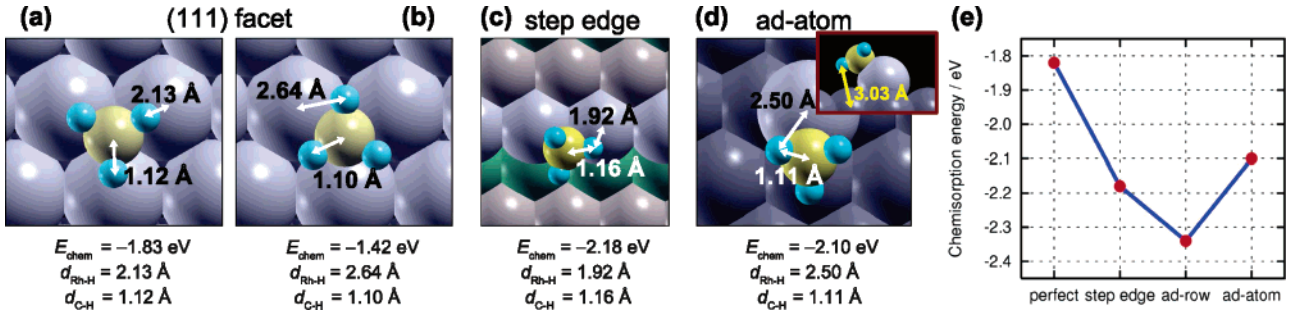


***Figure 3.*** (a,b) Adsorption geometry of a methyl radical at an fcc site of perfect Rh(111). In (a) the orientation of methyl is such that H atoms point toward the nearest metal atoms, while in (b) the H atoms point toward the hcp sites. (c) Methyl adsorption geometry at a step edge. Note that one H atom is pointing toward the step atom, thus exhibiting agostic C−H−metal bonding (the structure of methyl adsorbed at an ad-row is similar). (d) Methyl adsorption geometry at an ad-atom; note the large H−metal distance. (e) $CH_3$ adsorption energies for the best site at different reaction centers.

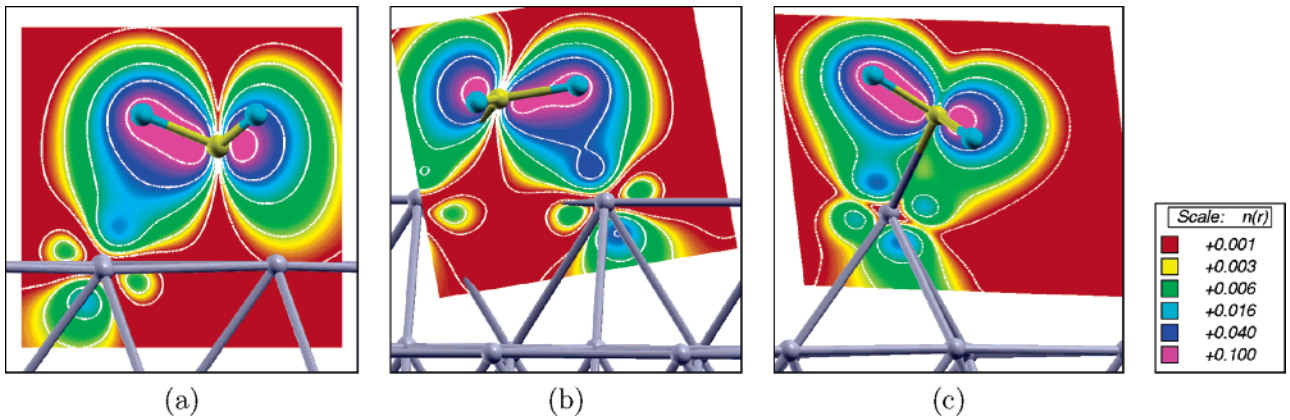


***Figure 4.*** Integrated local density of states (ILDOS, see text) illustrating the extent of three-center C−H−metal agostic bonding of methyl adsorbed on (a) a Rh(111) facet, (b) a step adge, and (c) an ad-atom. The magnitude of ILDOS increases from red to violet, following a rainbow scale. Five contours are drawn in logarithmic scale from $10^{-1}$ to $10^{-3}$ $e/a_0^3$.

The three-center C−H−metal bond results essentially from the hybridization of 1e CH bonding orbitals with the d-states of the metal surface.[22] In the case of methyl, such agostic bonds occur when the adsorption geometry allows for a small H−metal distance. On the (111) facet this happens when $CH_3$ is adsorbed onto a three-fold hollow site and oriented so that H atoms point toward the nearest metal atoms (see Figure 3a). The main effect of agostic bonding is to increase the chemisorption energy. Consider, for example, a methyl radical adsorbed at an fcc hollow site with H atoms pointing toward either the nearest metal atoms (thus giving rise to agostic bonds, Figure 3a) or the nearest hollow sites (no agostic bonds, Figure 3b). The difference between the two adsorption energies is rather large (∼0.4 eV); also note that, in the former case, the C−H distance is slightly larger than in the latter. The occurrence of agostic bonding may reverse the expected order of molecular stability at different adsorption sites. In the case of Rh(111), for instance, one would expect that the dangling bond of the $CH_3$ radical would most easily be saturated at a top site. Adsorption at a three-fold hollow site is instead slightly favored (the chemisorption energy is −1.83 eV, slightly more stable than −1.74 eV at the top site), provided the orientation is such as to allow for the formation of agostic bonds with neighboring metal atoms. Finally, agostic bonding may result in a stretched C−H distance and in a correspondingly weaker C−H bond. This effect is enhanced when going from the (111) facet to the step edge and ad-row (see Figures 3 and 4), while at an ad-atom defect the H−metal distance is quite large, indicating a smaller agostic interaction.

Some discrepancies exist in the literature about the site stability of methyl on Rh(111). Mavrikakis et al.[23] predicted the top site to be the most stable, with $E_{ads} = -1.84$ eV, and the fcc site to be 0.44 eV less bound. Note, however, that they only considered the orientation of methyl shown in Figure 3b, which we predict to be less stable (no agostic bonds). Walter et al. predicted the same adsorption structure as us,[24] but with a larger adsorption energy, $E_{ads} = -2.20$ eV. Our results are instead in good agreement with the results obtained by Xiao, $E_{ads} = -1.83$ eV[25] (see Supporting Information, Appendix B).

The nature of agostic bonding is illustrated in Figure 4, which displays the contour plots of the local density of states, integrated over an energy window (ILDOS) around the 1e molecular peak, which lies just below the metal d-band, approximately 7 eV below the Fermi level. Note that agostic bonding is stronger at a step edge (and also at an ad-row, not shown), where more charge is delocalized from the C−H bond toward the Rh atom. As a consequence, the C−H distance is increased to 1.16 Å (the bond weakens), while the H−Rh distance is shortened from 2.13 Å at a (111) facet to 1.92 Å. At an ad-atom the H−Rh distance is quite large (2.50 Å) due to the local geometry of the ad-atom defect, which hinders the formation of a strong agostic bond: methyl adsorbs on top of the ad-atom, forming

(22) (a) Michaelides, A.; Hu, P. *Surf. Sci.* **1999**, *437*, 362. (b) Papoian, G.; Nørskov, J. K.; Hoffmann, R. *J. Am. Chem. Soc.* **2000**, *122*, 4129.

(23) Mavrikakis, M.; Rempel, J.; Greeley, J.; Hansen, L. B.; Nørskov, J. K. *J. Chem. Phys.* **2002**, *117*, 6737.

(24) Walter, E. J.; Rappe, A. M. *Surf. Sci.* **2004**, *549*, 265.

(25) Xiao, H.; Xie, D. *Surf. Sci.* **2004**, *558*, 15.

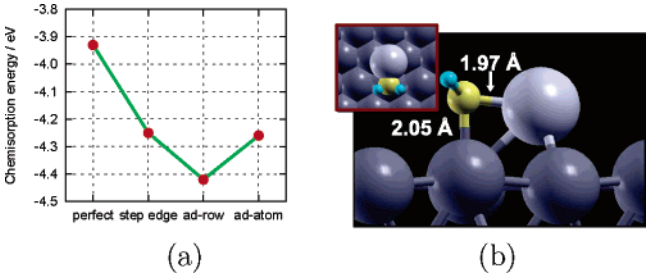


***Figure 5.*** (a) Adsorption energy, $E_{chem}$, of a $CH_2$ radical for different adsorption centers. (b) Structure of $CH_2$ adsorbed at an ad-atom center on Rh(111).

a tilted C−ad-atom bond. We have identified two almost degenerate $CH_3$ structures, where the methyl is rotated by ∼60° around the C−Rh bond axis (one structure is shown in Figure 3d, while the other is shown in Figure 4c). As shown in Figure 3d, the shortest H−Rh distance, 2.50 Å, is formed with the Rh ad-atom, while the distance between the bottom-most H atom and the surface Rh atom underneath is even larger, 3.03 Å, as shown in the inset of Figure 3d.

According to the Hammer−Nørskov chemisorption model,[26] the strength of molecule−surface bonds on late transition-metal surfaces is correlated to the center of the d-band of the surface metal atoms at the adsorption site: the higher the center of the d-band, the stronger the chemisorption energy. As a lower coordination of the surface metal atom results in a higher center of the local d-band (ligand effect), one would expect the methyl adsorption energy to increase when going from a (111) facet ($N_C = 9$) to a step edge ($N_C = 7$), an ad-row ($N_C = 5$), and finally an ad-atom ($N_C = 3$). Indeed, this is what happens in the first two cases, but at an ad-atom the methyl−surface binding decreases instead of further increasing (see Figure 3e). We interpret this behavior as being due to agostic bonds, which increase the magnitude of the adsorption energy on a (111) facet, a step edge, and an ad-row, while at an ad-atom the H−metal distance is too large for them to form (ensemble effect). On the other hand, the magnitude of the methyl adsorption energy at the top site—where agostic bonding is geometrically hindered—increases from a (111) facet to an ad-atom, as expected (see Figure 2). As agostic bonding weakens the C−H bond, thus helping break it, the ad-atom reaction center may not be the best for the second reaction, (2). The relation beween the strength of the C−H bond (as measured by the C−H stretching frequency) and the dehydrogenation barrier has also been discussed by Michaelides.[27]

In order to better understand why the $CH_3 \rightarrow CH_2 + H$ reaction is hindered at an ad-atom site, let us now discuss the adsorption of the products ($CH_2 + H$). At the TS the methylene radical is located close to a bridge site (Figure 1). In Figure 5 we display the $CH_2$ adsorption energy at this site for the four investigated reaction centers. The strength of the $CH_2$−surface bond increases on passing from a (111) facet to a step edge and an added row, as expected, because the coordination number of the metal atoms at the corresponding bridge sites decreases. At an ad-atom defect, the methylene radical bridges the ad-atom ($N_C = 3$) to a surface atom underneath ($N_C = 10$). The average coordination number of the two bridged atoms is thus $N_C = 6.5$, close to the value $N_C = 7$ of the step edge. As a result, the adsorption energies of methylene at an ad-atom and at a step edge are very similar: −4.26 and −4.25 eV, respectively. At a (111) facet, step edge, and ad-row, the two bonds formed by a methylene radical are equivalent, while at an ad-atom they differ: the bond with the ad-atom is strong, while that with the surface atom underneath is weak (see Figure 5b).

(26) Hammer, B.; Nørskov, J. K. *Adv. Catal.* **2000**, *45*, 71.
(27) Michaelides, A.; Hu, P. *J. Chem. Phys.* **2001**, *114*, 2523.

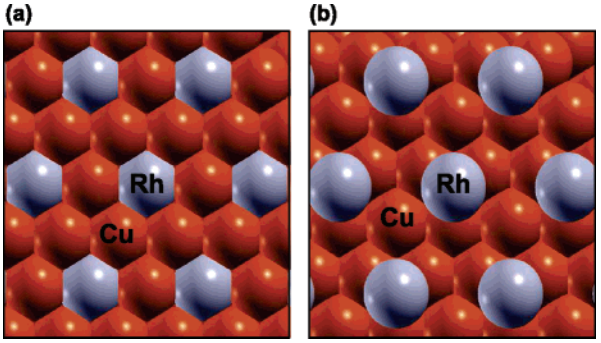


***Figure 6.*** Two newly designed reaction centers: (a) Rh atom substitutionally embeded into Cu(111) and (b) Rh ad-atom on Cu(111).

As for the H atom produced by the reaction, we have already mentioned that its adsorption energy is rather insensitive to the coordination of the metal reaction center. However, this is so only for the best adsorption sites corresponding to each reaction center: the hollow site at the (111) facet, the bridge site at the step edge and ad-row, and the ad-atom-to-surface bridge site for the ad-atom. At the TS of the $CH_3 \rightarrow CH_2 + H$ reaction, the H atom is located instead close to a top site (see Figure 1). The hydrogen adsorption energies on top of a metal atom are also rather similar when the reaction occurs at a (111) facet, at step edge, and at an ad-row (∼ −2.45 eV). When the reaction occurs at an ad-atom, instead, the adsorption of hydrogen over a top site is about 0.2 eV less stable. Therefore, the smaller binding of hydrogen to the metal site closest to the geometry of the $CH_3 \rightarrow CH_2 + H$ transition state also contributes to the large value of the activation energy when this reaction occurs at an ad-atom defect.

### 3. Design of an Optimized Reaction Center

The qualitative insight thus gained on the reactivity of different metal centers toward methane and methyl dehydrogenation can be used to design an optimal catalyst that would enhance the first reaction while hindering the second, possibly acting on the local chemical composition as well as on geometry. To achieve this goal, three requirements should be met: (i) one of the $CH_2$−metal bonds should be substantially weakened, (ii) the strength of the H−metal bond at the top site should be reduced, and (iii) agostic C−H−metal bonding of $CH_3$ should be prevented. Note that agostic interactions are small; hence, the effect of agostic bonding on the reaction barrier can only be small. On the other hand, the $CH_2$−surface and H−surface bonds are strong, and a large reduction of these bond strengths can affect the reaction barrier substantially. It turns out that the above requirements can be fulfilled more or less simultaneously.

Consider, for example, an isolated Rh atom substitutionally embedded into a Cu(111) surface (see Figure 6a). This can be seen as a model for a Cu-rich phase of a RhCu alloy. The C−Rh bond is roughly estimated to be ∼0.5 eV stronger than a C−Cu

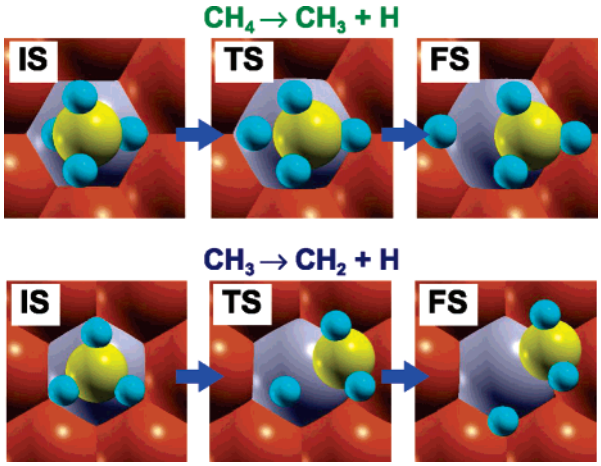


***Figure 7.*** Initial (IS), transition (TS), and final state (FS) structures for the first two steps of methane dehydrogenation over the Rh atom substitutionally embedded into Cu(111).

bond (see note 28 and Table S1 in the Supporting Information). The methylene radical produced by the dehydrogenation of methyl will thus form one strong bond with the substitutional Rh atom, while the other bond with a Cu atom will be much weaker. On the other hand, the strength of the H−surface bond at the top site (the high-symmetry site closest to the position of the H atom at the TS, see Figure 1) is very similar to that on Rh(111). As for the adsorption of methyl, we find that it prefers to adsorb on top of the Rh atom ($E_{ads} = -1.71$ eV), even if on both Rh(111) and Cu(111) it binds preferentially on an fcc hollow site (see Table S1). This is due to the fact that Rh is much more reactive than Cu (see note 29) and to the fact that, in this case, agostic bonding is not so strong as to favor the adsorption of $CH_3$ at the hollow site. The calculated reaction barrier for the first reaction, $CH_4 \rightarrow CH_3 + H$, is almost the same as that on perfect Rh(111) (0.70 vs 0.69 eV). On the other hand, the barrier for the second reaction is, as expected, substantially larger than that on Rh(111) (0.84 vs 0.42 eV). In fact, the barrier of 0.84 eV is even larger than that at a Rh ad-atom defect on Rh(111) (0.63 eV), thus confirming our qualitative picture. Snapshots of the two reactions are shown in Figure 7. Given that the two reaction barriers on clean Cu(111) are predicted to be 1.7 and 1.5 eV, the reactions would selectively occur near the Rh atom. Although the barrier for the second reaction, $CH_3 \rightarrow CH_2 + H$, is increased by a factor of 2 at the above reaction center, the difference in the activation barriers of the two reactions is small, ∼0.1 eV; tuning the chemical composition of the reaction center merely increases—albeit substantially—the barrier for the second reaction.

Somewhat related ideas about bimetallic catalysts have been used by Nørskov et al.[13,30] in their study of $CH_4$ activation and steam-reforming process. They showed that, by alloying Au into Ni, the chemisorption energy of carbon is substantially decreased, while the effect on the $CH_4$ activation is much smaller. These arguments were then used to design an improved steam-reforming catalyst, which contains a small amount of Au alloyed into Ni. There is, however, a noticeable difference between the two catalysts: the AuNi catalyst for steam reforming consists of individual inert atoms in a reactive substrate, whereas the above-discussed RhCu model catalyst consists of isolated reactive atoms embedded in an inert (or less reactive) substrate.

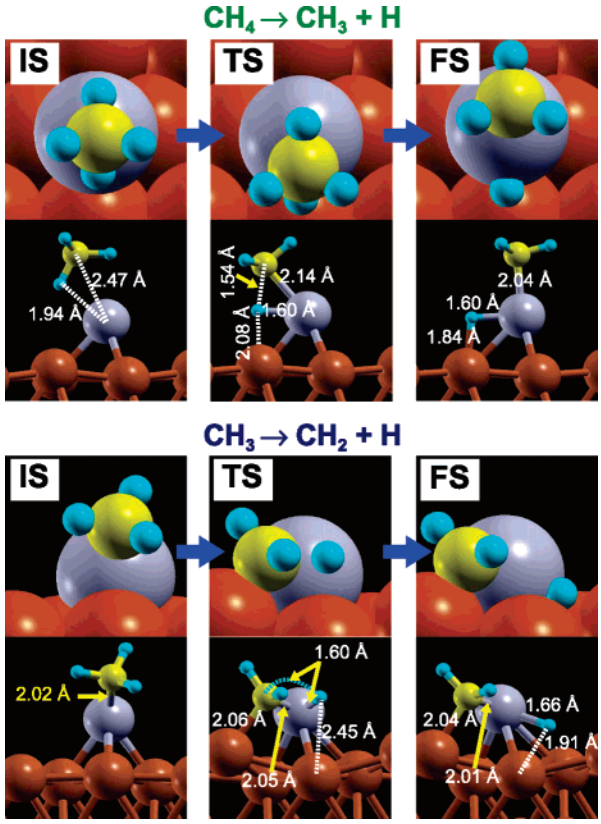


***Figure 8.*** IS, TS, and FS structures for the first two steps of methane dehydrogenation over the Rh ad-atom on the Cu(111).

By combining the structural effects described in section 2 with the chemical effects just outlined, it is possible to selectively enhance the barrier of the second reaction, while *reducing* that of the first. Consider, for example, a Rh ad-atom adsorbed onto a Cu(111) surface (see Figure 6b). In this case, the reaction barrier for the first reaction is very small, $E^* = 0.35$ eV, while the barrier for the second reaction is large, $E^* = 0.89$ eV. The snapshots for the two reactions on the Rh/Cu(111) center are shown in Figure 8. The C−H and H−Rh bond distances for the first reaction are similar to those obtained for Rh(111) (Figure 1). Moreover, the structures of the TS for the first reaction are also always similar, irrespective of the details of the reaction center, with C−H and the H−Rh bond lengths always around 1.6 Å. Indeed, these bond lengths are also close to those obtained for the oxidative addition of methane to metal complexes containing a single Rh atom.[31]

In terms of ligand and ensemble effects, the trend for the two reactions can be described as follows. The first reaction is insensitive to ensemble effects, because it requires only one reactive atom, but its barrier is reduced by ligand effects; for this reason, the less coordinated the reaction center, the smaller

(28) The difference in the bond strength of the C−Rh vs C−Cu single bond of adsorbed methylene on Rh(111) and Cu(111) can be roughly estimated from the adsorption energies of $CH_2$. The $E_{ads}$ are −4.07 and −2.99 eV for Rh(111) and Cu(111), respectively. As the $CH_2$ forms two bonds with the surface, the strength of a single C−metal bond is roughly half the magnitude of $E_{ads}$. Therefore, the C−Rh bond is stronger by ∼0.5 eV compared to C−Cu.

(29) The C−metal bond strength of adsorbed $CH_3$ on Rh(111) and Cu(111) can be roughly estimated from the $E_{ads}$ for the top site, which are −1.74 and −1.20 eV, respectively.

(30) Besenbacher, F.; Chorkendorff, I.; Clausen, B. S.; Hammer, B.; Molenbroek, A. M.; Nørskov, J. K.; Stensgaard, I. *Science* **1998**, *279*, 1913.

(31) Siegbahn, P. E. M. *J. Organomet. Chem.* **1995**, *491*, 231.

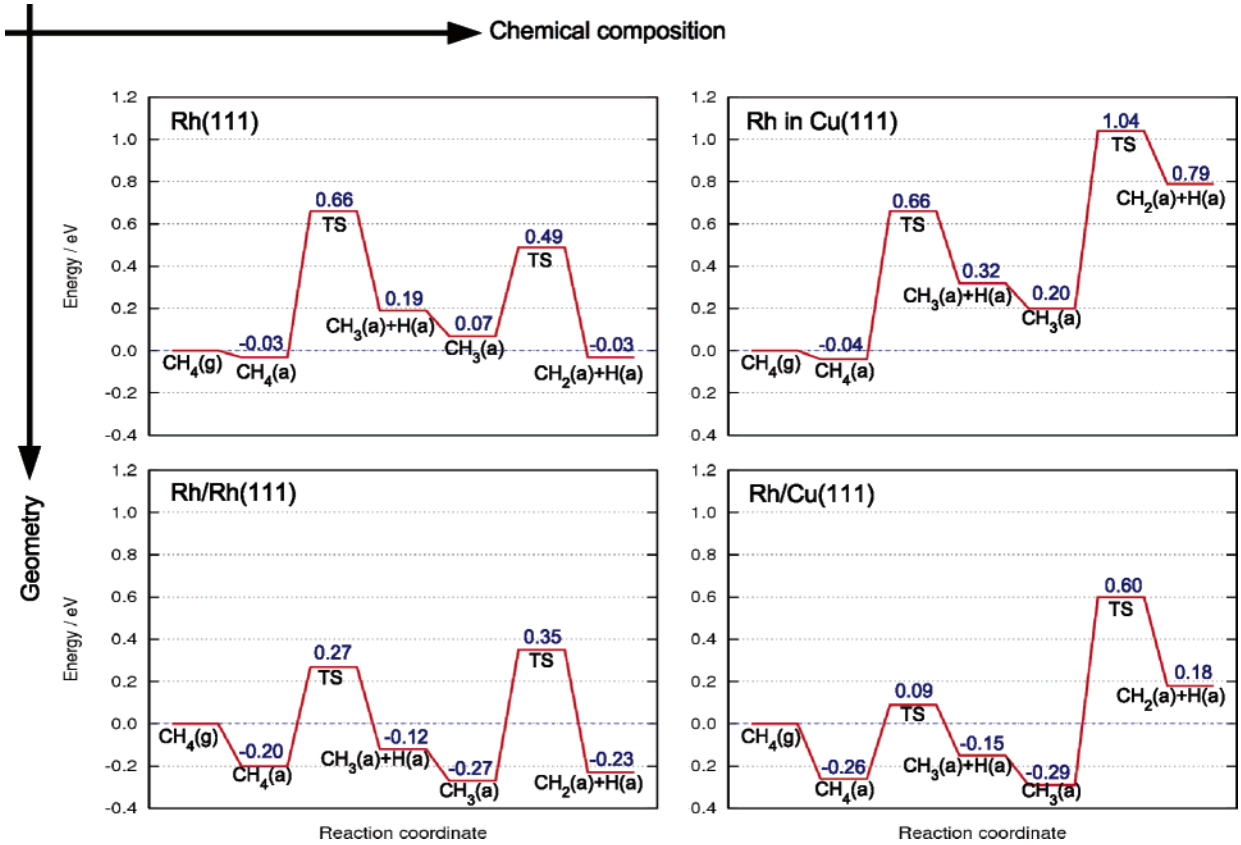


***Figure 9.*** Reaction profiles for the two dehydrogenation reactions at the reaction centers considered in Table 1. Arrows indicate the improved parameter of the reaction center. The zero level is the energy of the gas-phase methane. The difference between the labels "$CH_3(a) + H(a)$" and "$CH_3(a)$" is that, for the latter, the H(a) diffused to an equivalent site far from $CH_3(a)$.

the barrier. On the other hand, the second reaction is not that sensitive to ligand effects,[2] but it is very sensitive to ensemble effects: the barrier is substantially enhanced when the reaction center is composed of only one reactive atom. Moreover, the geometry of an ad-atom defect is such that ensemble effects are even stronger.

A catalytic device based on isolated metal ad-atoms, such as that shown in Figure 6b, is probably an academic model system, because the naked metal ad-atoms would either cluster or diffuse into the bulk. The problem is, of course, open on how to stabilize them. Even if it would be possible to stabilize them by some means, it is questionable whether such *stabilized* ad-atoms would still display the predicted unique properties. To shed some light on this question, we investigated the properties of a Rh ad-atom docked to chemisorbed atomic oxygen on Cu(111); such docking would stabilize the ad-atoms to some extent. Our calculations indicate that, even in this case, the activity of Rh ad-atoms would be selective: the barriers for the two reactions, (1) and (2), are 0.25 and 0.60 eV, respectively. One can also consider isolated metal atoms on some oxide support. For example, Zhang and Hu[32] predicted that the barrier for methane dehydrogenation near an isolated Pt ad-atom on a $MoO_3$(010) surface is significantly lower than that on Pt(111), while the further dehydrogenation of methyl is blocked.

In order to illustrate the combined effects of the local atomic structure and local chemical composition on the two dehydrogenation reactions considered in this paper, we summarize in Table 1 the reaction barriers for various reaction centers: perfect Rh(111), Rh ad-atom on Rh(111), Rh atom substituted in Cu(111), and Rh ad-atom on Cu(111). The corresponding reaction profiles are shown in Figure 9. The reference energy is the energy of the methane in the gas phase.

***Table 1.*** Activation Energies (in eV) for the First Two Steps of Methane Dehydrogenation

| reaction center (RC)[a] | improved parameter of RC | $E^*$ $CH_4 \rightarrow CH_3 + H$[b] | $E^*$ $CH_3 \rightarrow CH_2 + H$ |
|---|---|---|---|
| Rh(111) | | 0.69 | 0.42 |
| Rh/Rh(111) | geometry | 0.47 | 0.63 |
| Rh in Cu(111) | chemical composition | 0.70 | 0.84 |
| Rh/Cu(111) | geometry + chemical composition | 0.35 | 0.89 |

[a] Labels Rh/Rh(111), Rh in Cu(111), and Rh/Cu(111) stand for Rh ad-atom on Rh(111), Rh atom substitutionally embedded into Cu(111) (Figure 6a), and Rh ad-atom on Cu(111) (Figure 6b), respectively. [b] Activation energies for the first dehydrogenation with respect to adsorbed methane in the initial state.

## 4. Conclusions

A careful analysis of the results of computer simulations based on density-functional theory allows one to disentangle the mechanisms which determine the reactivity of a specific (model) catalyst at the nanometric scale. In the case of the first two dehydrogenation reactions of methane, on the basis of such an analysis, we predict that—by combining the effects of the local geometry and chemical composition at the active reaction center—isolated ad-atoms of a reactive catalyst, such as Rh, on a less reactive surface, such as Cu(111), should strongly favor the first reaction and hinder the second. Given that the two

(32) Zhang, C. J.; Hu, P. *J. Chem. Phys.* **2002**, *116*, 4281.

reaction barriers on clean Cu(111) are predicted to be 1.7 and 1.5 eV, our results indicate that these reactions would selectively occur at these specially designed centers, so that the methane dehydrogenation would be easily blocked after the first step. Of course, the problem is open on how to fabricate such nanostructured catalysts and how to stabilize them against ad-atom clustering or diffusion in the bulk. On the other hand, the other considered reaction center, composed of an isolated reactive atom substitutionally embedded into a less reactive metal, such as the Cu-rich phase of RhCu alloy, is more realistic and still possesses interesting properties, although not so pronounced as those of the ad-atom.

Small dispersed RhCu particles—a few nanometers in size—have been characterized on supports such as $Al_2O_3$[33,34] and $SiO_2$.[7,35] As for the bulk alloy, the phase diagram of RhCu shows two phases, a Rh-rich phase (with Cu concentration, $X_{Cu} \lesssim 0.1$) and a Cu-rich phase (with $X_{Cu} \gtrsim 0.8$).[36] However, on the surface, the amount of Cu is enriched; with just a small amount of Cu ($X_{Cu} > 0.05$), the Cu-rich phase will form on the surface.[33] The Cu-rich phase is compatible with a model catalyst considered in this paper, that is, isolated Rh atoms substitutionally embedded into Cu.

The model catalysts examined in this paper will probably turn out to be far too simplistic to be used in realistic conditions. We do believe, however, that the kind of arguments and analysis presented and utilized in the present paper will be instrumental to understanding the mechanisms responsible for the activity of real catalysts and to the design and realization of new materials with tailored catalytic properties.

**Acknowledgment.** This work has been supported in part by INFM through *Iniziativa trasversale calcolo parallelo* and by the Slovenian Research Agency (Grant No. P2-0148).

**Supporting Information Available:** Appendices A and B, as described in the text. This material is available free of charge via the Internet at http://pubs.acs.org.

JA060114W

(33) Chou, S.-C.; Yeh, C.-T.; Chang, T.-H. *J. Phys. Chem. B* **1997**, *101*, 5828.
(34) Fernandez-Garcia, M.; Martinez-Arias, A.; Rodriguez-Ramos, I.; Ferreira-Aparicio, P.; Guerrero-Ruiz, A. *Langmuir* **1999**, *15*, 5295.
(35) Coq, B.; Dutartre, R.; Figueras, F.; Rouco, A. *J. Phys. Chem.* **1989**, *93*, 4904.
(36) Massalski, T. B.; Okamoto, H.; Subramanian, P. R.; Kacprezak, L. *Binary Alloy Phase Diagrams*, 2nd ed.; ASM: Materials Park, OH, 1990.